Multisymbol Time Division Coding for High-Frequency Steady-State Visual Evoked Potential-Based Brain-Computer Interface

Xiaochen Ye, Chen Yang, *Member, IEEE*, Yonghao Chen, Yijun Wang, *Member, IEEE*, Xiaorong Gao, *Member, IEEE*, and Hongxin Zhang

***Abstract*— The optimization of coding stimulus is a crucial factor in the study of steady-state visual evoked potential (SSVEP)-based brain-computer interface(BCI).This study proposed an encoding approach named Multi-Symbol Time Division Coding (MSTDC). This approach is based on a protocol of maximizing the distance between neural responses, which aims to encode stimulation systems implementing any number of targets with finite stimulations of different frequencies and phases. Firstly, this study designed an SSVEP-based BCI system containing forty targets with this approach. The stimulation encoding of this system was achieved with four temporal-divided stimuli that adopt the same frequency of 30 Hz and different phases. During the online experiments of twelve subjects, this system achieved an average accuracy of 96.77 ± 2.47% and an average information transfer rate (ITR) of 119.05 ± 6.11 bits/min. This study also devised an SSVEP-based BCI system containing 72 targets and proposed a Template Splicing task-related component analysis (TRCA) algorithm that utilized the dataset of the previous system containing forty targets as the training dataset. The subjects acquired an average accuracy of 86.23 ± 7.75% and an average ITR of 95.68 ± 14.19 bits/min. It can be inferred that MSTDC can encode multiple targets with limited frequencies and phases of stimuli. Meanwhile, this protocol can be effortlessly expanded into other systems and sufficiently reduce the cost of collecting training data. This study provides a feasible technique for obtaining a comfortable SSVEP-based BCI with multiple targets while maintaining high information transfer rate.**

***Index Terms*— Brain-computer interface, steady-state visual evoked potential, time division coding, multi-target, high-frequency, phase modulation.**

Manuscript received June 21, 2021; revised October 31, 2021, January 28, 2022, and April 19, 2022; accepted May 10, 2022. Date of publication June 17, 2022; date of current version June 24, 2022. This work was supported in part by the National Natural Science Foundation of China under Grant 62006024, in part by the Fundamental Research Funds for the Central Universities Beijing University of Posts and Telecommunications (BUPT) under Project 2019XD17, in part by the Key Research and Development Program of Guangdong Province under Grant 2018B030339001, in part by the Aeronautical Science Foundation of China under Grant 2019ZG073001, and in part by the National Key Research and Development Program of China under Grant 2017YFB1002505. *(Xiaochen Ye and Chen Yang contributed equally to this work.) (Corresponding author: Hongxin Zhang.)*

This work involved human subjects or animals in its research. Approval of all ethical and experimental procedures and protocols was granted by the Tsinghua Institutional Review Board under Application No.20210032.

Xiaochen Ye, Chen Yang, and Hongxin Zhang are with the School of Electronic Engineering, Beijing University of Posts and Telecommunications, Beijing 100876, China (e-mail: hongxinzhang@bupt.edu.cn).

Yonghao Chen and Xiaorong Gao are with the Department of Biomedical Engineering, Tsinghua University, Beijing 100084, China.

Yijun Wang is with the Institute of Semiconductors, Chinese Academy of Sciences, Beijing 100083, China.

Digital Object Identifier 10.1109/TNSRE.2022.3183087

I. Introduction

BRAIN-COMPUTER interface (BCI) is an innovational human-computer interaction technique. It establishes a direct communication pathway between human and external devices without relying on peripheral muscles [1]. BCI systems have been widely used in medical and rehabilitation fields [2], [3]. Steady-state visual evoked potential (SSVEP)-based BCI, an influential paradigm of noninvasive BCI, has attracted considerable attention because of its high information transfer rate (ITR) and robustness. SSVEP is a distinctive neural response in the human brain, evoked by visual stimuli with fixed frequencies, and SSVEP responses in the visual cortex present stable features in the frequency domain [4]. Traditional SSVEP-based BCI usually comprised stimuli of different frequencies, so the BCI system can recognize the commands that the users wish to deliver by detecting the components of SSVEP responses in electroencephalogram (EEG) [5], [6].

Although the researches on SSVEP-based BCI develop rapidly, some tremendous difficulties still exist in the application area. Typically, how to devise a system implementing numerous targets; how to optimize stimulation paradigm [7]; how to enhance the comfortability of stimuli; how to reduce the fatigue of subjects [8] are critical questions that restrict the expansion of SSVEP-based BCI applications.

Multi-target SSVEP-based BCI is an important direction in the field of SSVEP-based BCI research. Researchers have tried to realize the SSVEP multi-target coding paradigm in a variety of ways. Yang *et al.* designed an SSVEP-based BCI system with 40 candidate targets based on frequency coding (8-15.8Hz, 0.2-Hz steps) [9]. Chen *et al.* proposed a method of hybrid frequency and phase coding, which can encode forty targets with eight stimulation frequencies (8-15Hz, 1-Hz steps) and five phases (0, 0.4π, 0.8π, 1.2π, 1.6π) [10]. However, it is challenging to encode numerous visual stimuli with frequency and phase modulation because the efficient frequencies of visual stimuli are limited, considering the human

body's physiological characteristics. To solve this problem, Zhang *et al.* introduced multiple frequencies sequential coding (MFSC), which combining time domain and frequency domain to achieve a 4 targets paradigm by two stimulation frequencies (7.5Hz, 12Hz) [11]. Time domain and frequency domain fusion coding is a good design idea, but a general solution for multi-target SSVEP-based BCI has not yet been proposed.

SSVEP-based BCI is one of the most robust and generalized BCI systems, but visual discomfort caused by stimulations is a key drawback in SSVEP-based BCI. In general, visual stimuli under low frequencies (less than 15Hz) will arouse stronger responses that are beneficial for detection. However, low-frequency stimuli also cause obvious visual discomfort; high-frequency stimuli (higher than 30Hz) will significantly trigger lesser discomfort at the risk of weaker responses [12], [13]. Many studies of high-frequency stimuli have been done. Chen *et al.* encoded 45 targets with 45 high frequencies (35.6-44.4Hz, 0.2Hz steps) [14]. Reference [15] encoded six targets with three frequencies (25, 33.3, 40 Hz). Reference [16] achieved encoding of four targets with the same frequency (60Hz) and four different phases (0, $\pi/2$, π, $3\pi/2$). Nevertheless, most of those studies only encoded limited targets, and the overall performance was relatively poor.

To eliminate those puzzles, we proposed a method named Multi-Symbol Time Division Coding (MSTDC). Refer to MFSC, MSTDC can encode any number of targets with a time-division sequence while only takes advantage of stimulation with few frequencies and phases. Different from MFSC, MSTDC is a method optimized to maximize the difference between the responses of different targets, and cannot only be used to encode symbols of different frequencies but also can further encode codes of different phases. This study first proposed a code set distance definition to evaluate the effectiveness of different code combinations. Secondly, an optimization method based on simulated annealing algorithm is designed to generate an optimized code set. Thirdly, applying stimuli of 30Hz frequency and four phases as basic symbols, this study developed 40 targets SSVEP-based BCI based on MSTDC and evaluate its efficiency through online experiments. Finally, we developed an online SSVEP-based BCI system implementing 72 targets and proposed a Template Splicing-TRCA algorithm. The result suggests that MSTDC can be easily expanded into the system of numerous targets, and the detection algorithm can significantly broaden the training template with only training datasets of few visual stimuli.

The structure of this paper is arranged as follow: the section II introduces the encoding method of MSTDC, the section III validates the efficiency of this method, the section IV introduces details about the SSVEP-based BCI system of forty targets, and the section V expands the number of targets into 72 and evaluates its scalability.

II. Encoding Method

A. Time-Division Encoding and Optimization Protocols

1) Concepts About MSTDC: This study proposed an encoding method called MSTDC, which is based on maximizing the difference between responses of stimulation, thus encoding any number of targets with a small number of symbols.

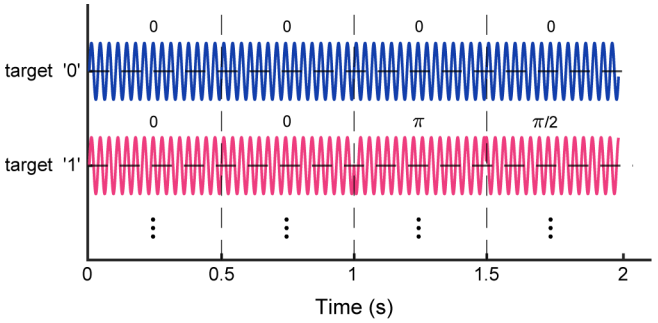

Fig. 1. The schematic diagram of codeword stimulus. The initial phase of the stimulus segment is marked on the top of the waveform.

(1) Symbol: symbol is the fundamental stimuli unit in this approach. It can be defined as any stimuli that can evoke stable neural responses in the human brain, while the responses caused by different symbols must be different. For example, it is possible to define 4 types of symbols $S_1 \sim S_4$: 30 Hz sine stimulation with initial phases of 0, $\pi/2$, π, and $3\pi/2$ respectively, and the stimulation duration of each symbol is 0.5 seconds.

(2) Codeword: codewords are primary combinations in MSTDC. Each codeword corresponds to a stimulus target. Codewords consist of several temporal divided symbols. The arrangements of codewords should be mutually exclusive. The number of symbols in a single codeword is defined as the length of codewords. For example, 4 symbols (the length of codewords=4) from $S_1 \sim S_4$ can be selected for permutation A total of $4^4 = 256$ kinds of codewords can be formed, which are respectively denoted as $C_1 \sim C_{256}$.

(3) Code set: Code sets are primary research objectives in MSTDC. Code sets are composed of all codeword arrangements. MSTDC is mainly applied to code sets of the same length. Thus all codewords should maintain the same length in every code set. For example, if a paradigm only needs 2 candidate targets, 2 codewords can be selected from all codewords ($C_1 \sim C_{256}$) as target '0' and target '1'. The schematic diagram of codeword stimulus is shown in Fig. 1.

(4) Symbol response, codeword response and code set response: the EEG responses evoked by symbols and codewords are called symbol responses and codeword responses respectively. Because codewords are temporal combinations of symbols, codeword responses can be acquired through fusion of symbol responses. All codeword responses are called code set responses. The relationship between those responses are shown in Fig. 2. The mathematical representations of those responses are shown in Table I. Where E represents the number of symbols, and $\boldsymbol{U}_e$ represents the average SSVEP responses evoked by e, N_s is the sampling points in a single trial. L is the length of codeword. $\boldsymbol{R}_n^{(l)}$ represents the responses evoked by l-th symbol in n-th codeword. N is the number of required codewords.

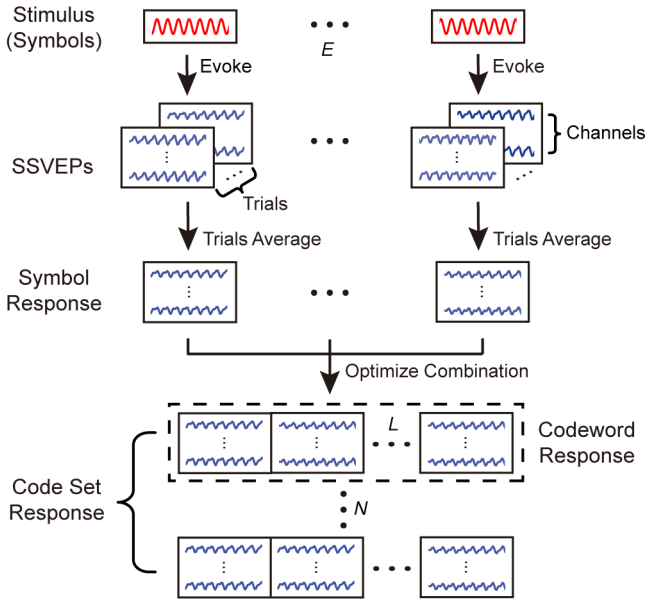

Fig. 2. The illustration of symbol, codeword and code set response.

TABLE I
MATHEMATICAL REPRESENTATION OF TERM DEFINITION

Definition	Mathematical Representations
Symbol response	$\boldsymbol{U}_e \in \mathbb{R}^{N_c \times N_s},\ e = 1,2,\ldots,E$
codeword response	$\boldsymbol{R}_n = [\boldsymbol{R}_n^{(1)}\ \boldsymbol{R}_n^{(2)}\ \cdots\ \boldsymbol{R}_n^{(L)}],\ \boldsymbol{R}_n^{(l)} \in \{\boldsymbol{U}_1, \boldsymbol{U}_2, \cdots, \boldsymbol{U}_E\}$
code set response	$\mathfrak{R} = \{\boldsymbol{R}_1, \boldsymbol{R}_2\ \cdots\ \boldsymbol{R}_N\}$

* {} denotes a set, [] denotes a new matrix composed of sub-matrixes by columns.

(5) Symbol response distance, codeword response distance, code set distance.

The symbol response distance is defined as the Euclidean distance between two symbol responses, which can be expressed as:

$$D_{\boldsymbol{U}_i \boldsymbol{U}_j} = \frac{1}{N_c} \left\| \boldsymbol{U}_i - \boldsymbol{U}_j \right\|_{\mathrm{F}}^2 \tag{1}$$

where $\|\cdot\|_{\mathrm{F}}^2$ represents Frobenius norm.

The codeword response distance, likewise, is defined as the Euclidean distance between two codeword responses, which can be expressed as:

$$D_{\boldsymbol{R}_i \boldsymbol{R}_j} = \left\| \boldsymbol{R}_i - \boldsymbol{R}_j \right\|_{\mathrm{F}}^2 = \frac{1}{N_c} \sum_{l=1}^{L} \left\| \boldsymbol{R}_i^{(l)} - \boldsymbol{R}_j^{(l)} \right\|_{\mathrm{F}}^2 \tag{2}$$

The code set distance was defined as the minimum distance between any two codeword responses, which can be calculated as follows:

$$\begin{aligned} D_{\mathfrak{R}} &= \min_{1 \le i < j <= N} D_{\boldsymbol{R}_i \boldsymbol{R}_j} \\ &= \min_{1 \le i < j <= N} \frac{1}{N_c} \sum_{l=1}^{L} \left\| \boldsymbol{R}_i^{(l)} - \boldsymbol{R}_j^{(l)} \right\|_{\mathrm{F}}^2 \end{aligned} \tag{3}$$

2) Objective Function of Optimization: Based upon utilizing average evoked responses across all subjects under different symbol stimuli, MSTDC maximizes the divisibility between all codewords in a code set by arranging the sequences of symbols. As a consequence, the primary goal of optimization in MSTDC is maximizing the code set distance through finding the optimal arrangements of symbol, which can be elaborated as follows:

$$\begin{aligned} \mathfrak{R}^* &= \arg\max_{\mathfrak{R}} D_{\mathfrak{R}} \\ &= \underset{\boldsymbol{R}_i^{(l)}, \boldsymbol{R}_j^{(l)} \in \{\boldsymbol{U}_1 \cdots \boldsymbol{U}_E\}}{\operatorname{argmax}} \ \min_{1 \le i < j <= N} \frac{1}{N_c} \sum_{l=1}^{L} \left\| \boldsymbol{R}_i^{(l)} - \boldsymbol{R}_j^{(l)} \right\|_{\mathrm{F}}^2 \end{aligned} \tag{4}$$

B. Optimization Algorithm

The optimal selections of template sets can be acquired through solving the optimization problem. Similar to the discrete p-dispersion problem discussed in [17], under the restriction of maximizing the minimum distance, the optimization of the code set is supposed to be an NP-complete problem. Thus, this optimal answer cannot be found with polynomial time. To address this problem, this study adopted Simulated Annealing (SA) [18] to find the approximate optimal solution.

The process of SA algorithm is demonstrated in Fig. 3, and the implementation process is shown as following:

Step 1: Setting the initial temperature T_{init}, the cut-off temperature T_{end}, the maximum number of iteration $iter_{max}$. The current temperature T is equal to the initial temperature, and the current number of iteration $iter$ is zero. Besides, an initial code set $\mathfrak{C}_{init}$ is built.

Step 2: Generating a new code set $\mathfrak{C}_{new}$

Step 2.1: Randomly generating a new codeword that doesn't belong to the current code set.

Step 2.2: Randomly selecting a codeword from the current code set.

Step 2.3: Exchanging the two codewords. The switched code set is defined as new code set.

Step 3: The algorithm decides whether to accept the new code set according to Metropolis criteria [18]. Repeating Step 2 until reaching the maximum number of iterations, and this algorithm jump to Step 4.

Step 3.1: Separately calculating the distances of two code set response D_{cur} and D_{new}.

Step 3.2: When $D_{new} > D_{cur}$, the new code set replaces the current code set.

Step 3.3: When $D_{new} < D_{cur}$, the new code set replaces the current code set with a fixed probability.

Step 4: Updating the current temperature T, if the temperature doesn't achieve the cut-off temperature, the system switches to Step 2. Otherwise, the result is outputted.

Table II shows the 'pseudo code' of this algorithm. The function Distance() is designed for evaluating code set distance, and the function UpdateCodeset() is designed for acquiring new code set. The initial temperature T_{init} is $1000 \times L$, the cut-off temperature T_{end} is 0.001, and the maximum number of iteration $iter_{max}$ is 500.

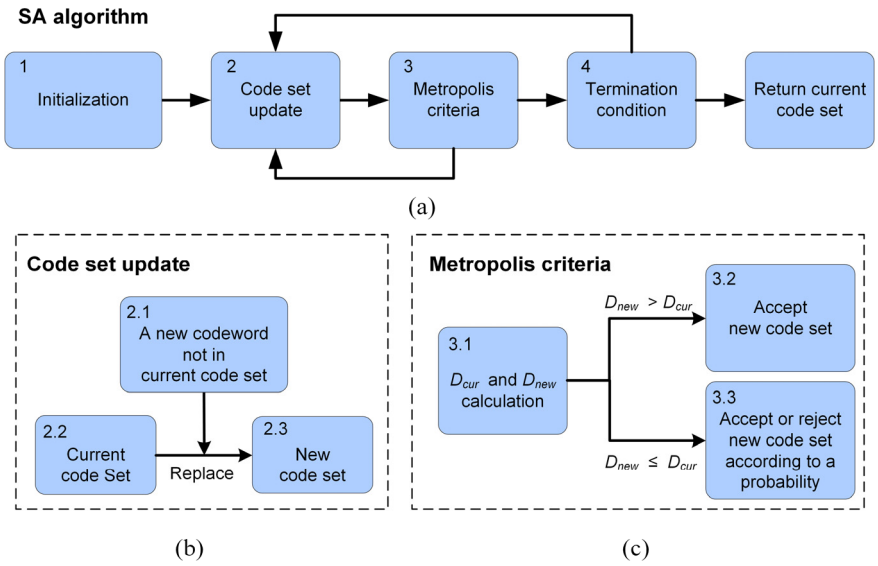

Fig. 3. The illustration of SA algorithm (a) Main framework; (b) Schematic diagram of code set update; (c) Schematic diagram of Metropolis criteria.

TABLE II
THE PROCESS OF APPLYING SA ALGORITHM ON OPTIMIZATION OF THE CODE SET

Algorithm 1 SA Algorithm

Initialize $\mathfrak{C}_{cur} \leftarrow \mathfrak{C}_{init}$, $T \leftarrow T_{init}$, $iter_{max}$
For $T \in [T_{end}, T_{init}]$ do
  $D_{cur} = \text{Distance}(\mathfrak{C}_{cur})$
  For $iter \in [1, iter_{max}]$ do
    $\mathfrak{C}_{new} = \text{UpdateCodeset}(\mathfrak{C}_{cur})$
    $D_{new} = \text{Distance}(\mathfrak{C}_{new})$
    $\Delta D \leftarrow D_{new} - D_{cur}$
    If $\Delta D > 0$ or $\exp(\Delta D/T) > \text{rand}(0,1)$ then
      $\mathfrak{C}_{cur} \leftarrow \mathfrak{C}_{new}$
    End if
  End for
  $T \leftarrow T \times 0.99$
End for
Return $\mathfrak{C}_{cur}$

TABLE III
EXPERIMENTAL COMPARISON TABLE

Experiment	First appearance	description
A-Offline	Section III.A	Basic data for code set optimization [16]
B-Offline	Section III.B	MSDTC validity verification experiment
SA-Codeset	Section III.B.1)	the optimal code set through the simulated annealing algorithm
RO-Codeset	Section III.B.1)	The code set with the largest code set distance in 10 million randomly generated code sets
C-Offline	Section IV.A.1)	The offline experiment with 40 targets based on SA-Codeset
C-Online	Section IV.A.1)	The online experiment with 40 targets based on SA-Codeset
D-Online	Section V.B	The online experiment with 72 targets based on SA-Codeset and TS-TRCA algorithm

III. VALIDATION OF THE ENCODING APPROACH

A. Estimation of Codeword Response

MSTDC considers the code word response as the fundamental component in the optimization method, so EEG data from different subjects is required as an optimized data set. A dataset, named Experiment A-Offline, was introduced to help optimizing the code set. (Experimental comparison table is shown in Table III)

This dataset was based on experiments of 4-target SSVEP-based BCI, including EEG data of ten subjects under 30Hz stimulus frequency and four kinds of phase (0, $\pi/2$, π, $3\pi/2$) [16]. All subjects were requested to fulfill the experiments of five blocks, while every block consists of 16 trials (four trials under each condition). Each trial lasted for 5s, containing 1s of inter-trial gaze shift and 4s of visual stimuli. The original sampling rate of this dataset was 1000Hz.

This research used 4 kinds of sinusoidal stimulus signals (frequency was 30Hz, initial phases were 0, $\pi/2$, π, $3\pi/2$) as the basic code elements. Nine channels in the occipital region (Pz, PO5, PO3, POz, PO4, PO6, O1, Oz, O2) were chosen to extract the symbol responses. In the preprocessing stage, the data was down sampled to 250 Hz, and a 50Hz notch filter was used to eliminate the noise. Besides, two band pass filters on 28-32Hz and 58-62Hz were used to extract the base frequency and second harmonics of SSVEP responses.

Individual templates under different visual stimuli can be acquired by averaging the SSVEP response of each subject. Moreover, the global symbol response was acquired through averaging individual templates.

This study estimated the distances between symbol responses in Experiment A-Offline dataset from 0.25s to 0.5s, as shown in Fig. 3. It can be inferred that the symbol response distance between two symbols with π of phase difference is

higher than two symbols with $\pi/2$ of phase difference, which corresponds to the visual stimuli itself. However, comparing the 0, $3\pi/2$ phase code response distance (325.5) and the π, $3\pi/2$ phase code response distance (231.5) under the condition of 0.5s; It can be found that although the symbol stimulation is equally spaced by $\pi/2$ phase, the distance difference between different symbol responses is enormous. Using symbols with a more considerable symbol response distance for encoding can effectively improve the distinguishability between codewords.

B. Encoding Validation Experiments

1) Paradigm Design: In order to validate the effectiveness of MSTDC, this study proposed a series of experiments (Experiment B-Offline) for validation. By estimating the result of Experiment A-Offline symbol response, the optimal code set arrangement (SA-Codeset) is selected through the simulated annealing algorithm. Meanwhile, deriving from ten million kinds of a randomly generated code set, a specific code set (RO-Codeset) enabling the largest code set response distance was chosen. It should be specially pointed out that both SA-Codeset and RO-Codeset use 0.5s as a single symbol length in the optimization process, and the corresponding codeword length is 2s.Under the condition of 4 types of symbols (0, $\pi/2$, π, $3\pi/2$), 4 bits of symbols can form a total of $4^4 = 256$ types of codewords. Randomly select 40 codewords from 256 types of codewords to form a code set, repeatedly generate 10^7 code sets, and select the one with the largest code set distance as the RO-Codeset. RO-Codeset will be performed as a control group experiment to verify the optimization effect of SA-Codeset.

The sine sampling approach [19] was implemented in this study, presenting forty visual stimuli on a 24.5-inch LCD monitor. The monitor is Alienware AW2518H with a refreshing rate of 240Hz and a resolution of 1920×1080.

Every visual stimulus corresponded to a codeword in the code set, every stimulus sequence consisted of four symbols ($L = 4$). Every symbol lasted for 0.5s with the stimulation frequency of 30Hz. The candidate symbol element contains a total of 4 phase-coded symbol element stimuli (0, $\pi/2$, π, $3\pi/2$), and the brightness during the stimulation process was fluctuated according to a sine function (Sine). During the stimulation process, a trigger signal was recorded at the onset of symbol presentation. The waveform of codeword stimulus brightness is shown in Fig. 1.

The experiment adopted the form of a cue-guided target selection task, simulating the online experiment to record data for offline analysis. SA-Codeset and RO-Codeset both recorded four blocks of data in an interleaved way. Every block contained forty trials, and each trial lasted for 3s. In each trial, the subjects were asked to follow the visual cue (the red box surrounding the target) to gaze at the target, and forty targets were scanned in a random order. At the beginning of a trial, the visual cue lasted for 1s, then users shift their attention on the stimuli target. During this time, all targets were not flashing. All stimuli began to flicker after the visual cue lasted for 1s, and a red triangle was given at the bottom of the required stimulus square, the stimulation phase lasted for 2s (0.5s per symbols). The users were requested to avoid eye blinking during visual stimuli, and the interval between block was 2 minutes.

2) Data Acquisition: Experiment B-Offline adopted the Neusen W system (Neuracle, Inc) to record EEG data. Nine electrodes (Pz, PO5, PO3, POz, PO4, PO6, O1, Oz, O2) were placed at the occipital region, and the reference electrode was placed at the crown of the head. Impedances of all electrodes were maintained lower than 10kΩ. Meanwhile, the sampling rate is 1000Hz, but the data were down sampled to 250Hz after being recorded. A 50Hz notch filter was introduced to eliminate power line noises.

Twelve subjects (five females and seven males, age 20-25) with normal or corrected-to-normal vision participated in the experiments. Every subject read and signed the informed consent. Every subject received financial rewards after the experiments. All experiments in this study were approved by the Tsinghua Institutional Review Board.

3) Data Analysis and Evaluation Criteria: Standard TRCA [20] is the detection algorithm in Experiment B-Offline. In the calculation process, two band-pass filters of 28-32 Hz and 58-62 Hz were used to extract the fundamental and the second harmonics components of the SSVEP response, and the weights of the two filters were both set to 1. Other parameters maintained the same with study [20].

In order to reduce the negative effect of the incubation period, all induced SSVEP responses were intercepted with a delay of 0.14s [20]. Leave-one-block-out was enabled in the analysis process, and the integrated results were computed with four cycles.

Detection accuracy and information transfer rate (ITR) were the primary evaluation indexes, to compare the detection efficiency of SA-Codeset and RO-Codeset. ITR was defined as:

$$ITR = \left(\log_2 N + log_2 P + (1-P) log_2 \left(\frac{1-P}{N-1}\right)\right) * \left(\frac{60}{T}\right) \tag{5}$$

where N is the number of targets, P is the average classification accuracy, T is the average detection time that contains the time of codeword stimulation and 0.5s for the inter-trial rest.

C. Result of Encoding Validation Experiments

1) Symbol Response Distance: The average symbol response distance was shown in Fig. 5. By comparing Fig. 4 and Fig. 5, it can be found that the symbol response distance between the two datasets is maintained similarly. The code response distance under the π-phase stimulation was mostly higher than the code response distance under the $\pi/2$ phase stimulus. But for Fig. 5, the distance between the 0-phase symbol response and the $3\pi/2$-phase symbol response is huge, and it has even exceeded the symbol response distance under the interval π-phase stimulus. Those phenomena may be caused by the experimental paradigm. During the Experiment B-Offline, the stage for reminding the target will start per 2s, and all targets maintained the highest brightness, which

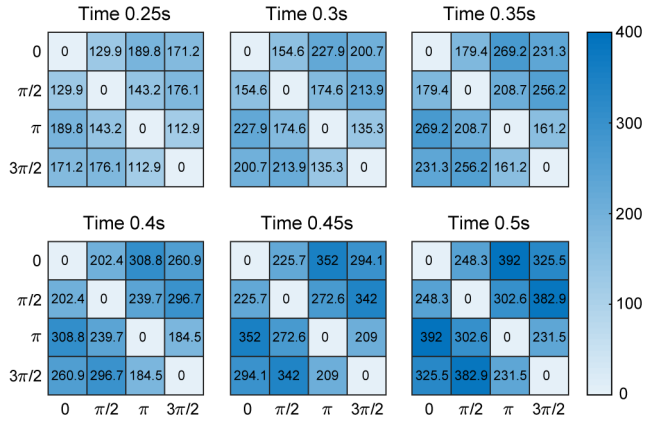

Fig. 4. Distances between symbol responses in Experiment A-offline dataset from 0.25s to 0.5s.

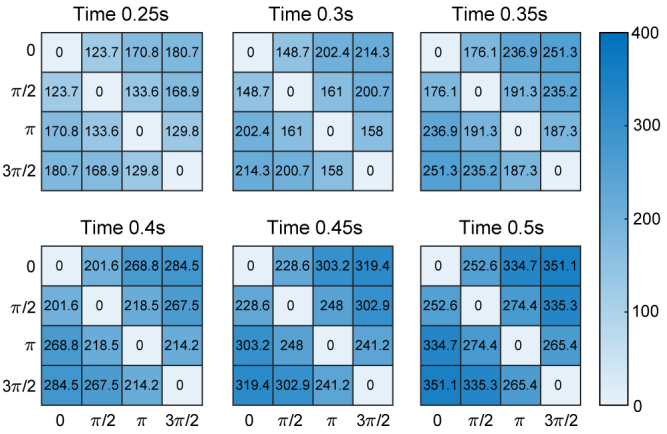

Fig. 5. The average symbol response distance in Experiment B-Offline dataset from 0.25s to 0.5s.

is similar to the symbol stimulus of the $\pi/2$ phase. Consequently, transient-state responses (TSR) may exist at the beginning stage of stimulation [21], resulting in errors in estimating symbol response distance. However, according to the results of following experiments, the overall performance of this encoding proposal didn't reduce, despite some symbol response distance were different in Fig. 4 and Fig. 5.

2) The Code Set Response Distance: This study intercepted symbols of different lengths at Experiment B-Offline dataset to investigate the performance difference under different lengths of symbols. For instance, if we extracted the symbol response data of 0.25s, which means 0.25s of data of every symbol was cut from the starting point, while a codeword response consisted of four symbols, so the length of the eventual codeword response was 1s.

Then we tested the responses of all subjects in the Experiment B-Offline experimental data set. According to the response distance defined by equation (3), the individual data of each subject is used as the unit to calculate the response distance of each subject in SA-Codeset and RO-Codeset in Experiment B-Offline. The results are shown in Fig. 6. The average response distance of SA-Codeset were superior than RO-Codeset, and the standard deviation on subjects were lower.

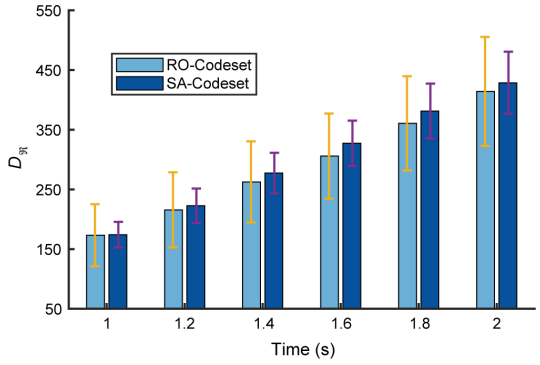

Fig. 6. Average code set response distance of Experiment B-Offline under different data lengths.

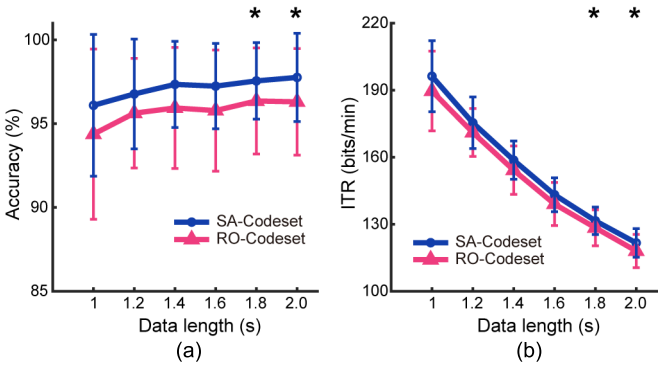

Fig. 7. Comparison of the two coding principles performance in the Experiment B-Offline data set. (a) classification accuracy (b) information transfer rate under different code lengths (data length intercepted by each symbol *4). The error bar in the figure represents the standard deviation between subjects. The asterisks in both figures indicate significant difference between the two code sets obtained by paired t-tests (*p<0.05).

3) Classification Accuracy and ITR: Fig. 7 shows the average classification accuracy and the ideal ITR of the two code sets when the codeword length is 1s-2s (corresponding symbol length is 0.25s-0.5s). When length is 2s, the average accuracy of SA-Codeset is 97.76%, the average ITR is 121.63 bits/min. Compared to RO-Codeset, the average accuracy and ITR achieved by SA-Codeset were much higher (paired t-tests on all subjects, ITR: p-value = 0.0159, Accuracy: p-value = 0.0184). The average classification accuracy increased as the length of the selected data increases, but the ideal ITR followed the opposite trend. The comparison results of the two code sets show that the optimized code set SA-Codeset performance was better than RO-Codeset when data of any length is selected. Especially when the data length is 1s, the average accuracy rate was increased by 1.72% relative to RO-Codeset, and the ITR was increased by 6.64 bits/min.

In order to improve the recognition accuracy and verify the impact of the codeword distance on the recognition result, 0.5s was chosen as the basic symbol duration of the online experiment in the follow-up research.

IV. Encoding Application

A. Encoding Application Experiments

1) Paradigm Design: In order to verify the application effectiveness of the Experiment B-Offline coding principle,

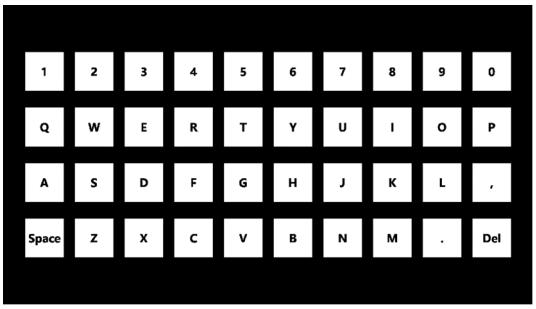

Fig. 8. Stimulation interface of Experiment C-Offline and Online.

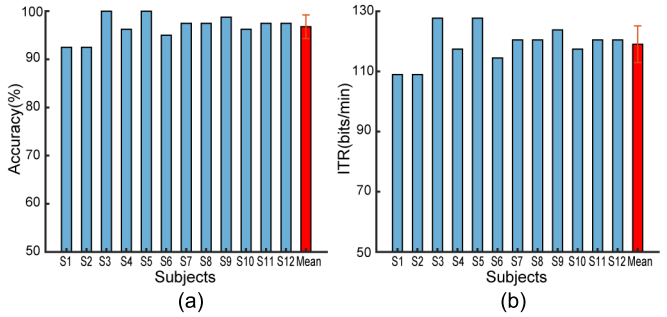

Fig. 9. Online recognition results of all subjects in the Experiment C-Online data set (a) Recognition accuracy (b) ITR.

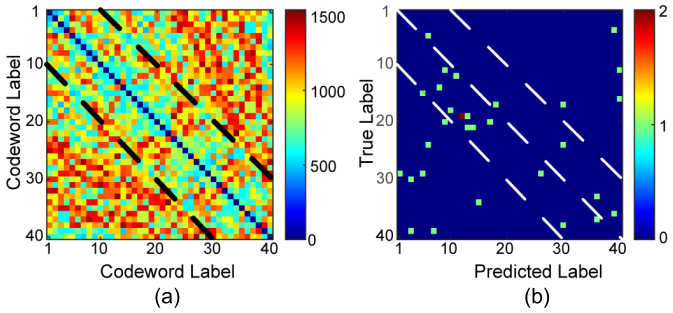

Fig. 10. The relationship between codeword distance and misjudgment trials in Experiment C-Online. (a) A distance matrix of 40 target codewords based on the encoded data set; (b) A matrix of misjudgments in online experiments of all subjects. The order of codewords is sorted according to the minimum distance between codewords to ensure that the minimum distance between any codewords is on both sides of the diagonal.

this study designed Experiment C-Offline and Experiment C-Online. In Experiment C-Offline and Experiment C-Online, SA-Codeset was used as the 40-target coding scheme, and the code word stimulus design was the same as described in section III.B. To simulate the spelling situation, this study designed the interface layout as shown in Fig. 8. Every stimulus square was presented with 140×140 pixels. The adjacent target has a horizontal spacing of 40 pixels and vertical spacing of 60 pixels.

Experiment C-Offline adopted the cue-select task paradigm, and each participant participates in 4 blocks experiment. Each block contained 41 trials, and the first trial is used to remind subjects that its data does not participate in the evaluation of results. Except for the first trial, each target was highlighted once in random order. Subjects need to focus on the cued target. At the beginning of each trial, a cue appeared and lasted for 1 second. All the targets began to blink at the same time and lasted for 2 seconds. During the simulation, the subjects were asked to avoid blinking. In order to reduce the effect of visual fatigue, a 2-minute rest period was arranged for the subjects between the blocks.

The Experiment C-Online experiment still used the cue-select task paradigm, and a total of 2 block experiments were carried out. The experiment process was the same as Experiment C-Offline. Experiment C-Online is scheduled after Experiment C-Offline. In the online experiment, the TRCA algorithm with Experiment C-Offline data as calibration data was used for EEG real-time analysis and feedback. The overall experimental process of Experiment C-Online is the same as that of Experiment C-Offline experiment. But in the online experiment, the system analyzes participants' EEG data in real time and provides feedback on the results after the stimulation phase. The recognition results will be presented in blue for feedback to the subjects, and the duration of each trial feedback phase is randomly about 0.5-1.25s.

Still, the system will analyze the participants' EEG data in real-time and give feedback on the results after the stimulation phase. The duration of the feedback phase was 0.5s, during which the judgment result will be rendered in blue for feedback to the subjects.

2) Data Acquisition and Analysis: Twelve subjects (six females and six males, age 20-25) with normal or corrected-to-normal vision participated in the experiments. Every subject read and signed the informed consent. Every subject received financial rewards after the experiments. All subjects took part in both offline experiments (Experiment C-Offline) and online experiments (Experiment C-Online). The recorded data in Experiment C-Offline was used as the source of training data in Experiment C-Online by TRCA algorithm, the spatial filters and individual templates of code set were implemented during the online experiments.

B. Encoding Application Experiment Results

1) Detection Accuracy and ITR: Results of Experiment C-Online show that the high-frequency phase-encoded forty-target SSVEP-based BCI application system had a high recognition efficiency, as shown in Fig. 9. With the standard TRCA as the recognition algorithm, twelve subjects achieved average recognition accuracy of 96.77%±2.47% and an average ITR of 119.05±6.11 bits/min. During the experiment, all subjects achieved a recognition accuracy rate of more than 90%, of which ten subjects achieved a recognition accuracy rate of more than 95%. It is worth noting that the recognition accuracy rates of S3 and S5 even reached 100%. From the perspective of ITR, twelve subjects achieved an ITR of more than 100 bits/min under the stimulation of high-frequency SSVEP, of which seven subjects had an ITR of more than 120 bits/min. The results suggested that the online system can achieve a significant ITR under relatively comfortable high-frequency stimulation conditions.

2) The Relationship Between Codeword Distance and False Positive Rate: Fig. 10 reflects the relationship between the

error detection and the codeword distance in Experiment C-Online, and the code word distance was cumulatively computed according to the forty targets encoding principle. The 40 codewords in Fig. 10 were sorted according to the distance between the codewords. To be more specific, the codeword with the smallest distance between the current codewords is selected as the next codeword. It can be seen from Fig. 10(a) that through this sorting method, the minimum distance between codewords will be concentrated on both sides of the main diagonal, while the more considerable code distance will be far away from the main diagonal of the codeword distance matrix. Fig. 10(b) reflects the misjudgment of the code word in the online experiment. It can be seen that the misjudgment is also concentrated on both sides of the main diagonal, where the codeword distance is relatively close.

V. Research on Application of Augmented Targets

A. Template Splicing-TRCA Algorithm

MSTDC can encode a large number of targets through encoding codewords. This characteristic allows each target to maintain the overall difference while retaining a strong correlation between the partial components. As demonstrated in II.A, a codeword consists of several symbols. Thus, the response can be approximately estimated through combinations of symbol responses. So the templates of responses can be acquired through sequential connections of symbol response templates. This study designed a Template Splicing-TRCA (TS-TRCA) that builds all codeword response templates based on symbol response templates. This method can adaptively modify the coding set through a training dataset, resulting in lower costs for the transfer training.

The response data for the n-th codeword in the base code set was denoted as $\boldsymbol{X}_n \in \mathbb{R}^{N_c \times N_s}$. Here, N_c is the number of channels, N_s is the number of sampling points in each trial. The filter bank analysis was introduced, decomposing the data into multiple sub-bands to extract the SSVEP harmonic components [23]. After applying m-th sub-band filter, $\boldsymbol{X}_n^{(m)}$ was obtained from $\boldsymbol{X}_n$. $\boldsymbol{X}_n^{(m)}$ was segmented by the symbol length, then the segments of data were categorized according to the symbol sequence in the corresponding word. The symbol template $\bar{\boldsymbol{U}}_e^{(m)} \in \mathbb{R}^{N_c \times N_{ss}}$ of symbol e was obtained by averaging multiple segments of response data. Here N_{ss} is the number of sampling points in each segment.

The k-th codeword in the augmented code set was denoted as $\mu_k \in \mathbb{Z}^L$. Here, k indicates the codeword index, L is the length of codeword. According to symbol sequence in codeword μ_k, the corresponding symbol templates were spliced. The codeword template of k-th codeword in the augmented code set was defined as

$$\bar{\boldsymbol{R}}_k^{(m)} = [\bar{\boldsymbol{U}}_{\mu_1}^{(m)} \bar{\boldsymbol{U}}_{\mu_2}^{(m)} \cdots \bar{\boldsymbol{U}}_{\mu_L}^{(m)}] \tag{6}$$

The process of calculating the ensemble spatial filter with the response data of the base code set and the codeword template data of the augmented code set is as follows:

Define

$$\boldsymbol{S}_k^{(m)} = \bar{\boldsymbol{R}}_k^{(m)} (\bar{\boldsymbol{R}}_k^{(m)})^T \tag{7}$$

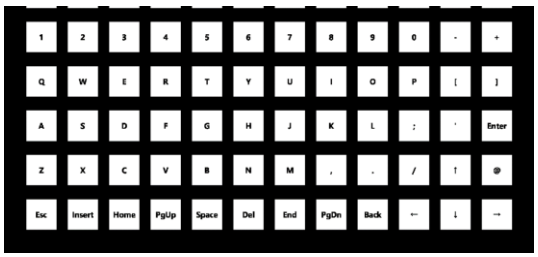

Fig. 11. Stimulation interface of Experiment D-Online.

All trials of response data in the base code set were sorted into a concatenated matrix in columns $\widehat{\boldsymbol{X}}^{(m)} = [\boldsymbol{X}_1^{1(m)} \cdots \boldsymbol{X}_1^{N_t(m)} \boldsymbol{X}_2^{1(m)} \cdots \boldsymbol{X}_2^{N_t(m)} \cdots \boldsymbol{X}_N^{1(m)} \cdots \boldsymbol{X}_N^{N_t(m)}]$. Here, m is the sub-band index. Each channel of data was centered.

Define

$$\boldsymbol{Q}^{(m)} = \widehat{\boldsymbol{X}}^{(m)} (\widehat{\boldsymbol{X}}^{(m)})^T \tag{8}$$

Spatial filters for the k-th codeword in the augmented code set was calculated as

$$\boldsymbol{w}_k^{(m)} = \underset{\boldsymbol{w}}{\operatorname{argmax}} \frac{\boldsymbol{w}^T \boldsymbol{S}_k^{(m)} \boldsymbol{w}}{\boldsymbol{w}^T \boldsymbol{Q}^{(m)} \boldsymbol{w}} \tag{9}$$

The ensemble spatial filter for all codewords was denoted as $\boldsymbol{W}^{(m)} = [\boldsymbol{w}_1^{(m)} \boldsymbol{w}_2^{(m)} \cdots \boldsymbol{w}_K^{(m)}]$. Here, K is the number of codewords in augmented code set.

As described in section III.B, the classification process of the test data was conducted with the ensemble spatial filter and codeword templates.

B. Experiments for Augmented Targets

To validate the feasibility of TS-TRCA, this study designed Experiment D-Online for augmented targets. The experiments in this group were carried out at the same time as the experiment in section IV, and the two groups of experiments were internally alternated with blocks.

1) Paradigm Design: According to Experiment A-Offline, this experiment designed a system implementing 72 targets by MSTDC. The length of codeword $L = 5$, and the duration of symbol was also 0.5s. The stimulation interfaces are shown in Fig. 11. A single codeword stimulus was set as a rectangular area of 110×110 pixels, targets had a horizontal distance of 40 pixels and a vertical distance of 50 pixels between each other.

Experiment D-Online and Experiment C-Online were hold in a staggered way, and they shared a same experiment procedure. All participants in Experiment C-Online also took part in the Experiment D-Online.

The Experiment D-Online experiment contained two blocks, and all 72 targets were prompted once in a random order, so each block experiment contained 72 trials. At the beginning of each trial, the cues target was selected by a red frame to help the subject gazing at the target, and the cue time lasted for 1 second. After the prompt is over, all targets start flashing simultaneously, and the flashing time lasts for 2.5s. After

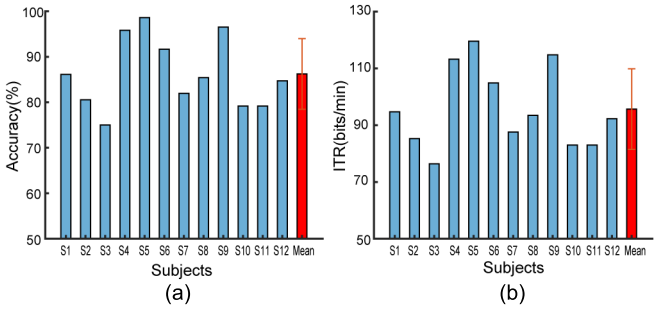

Fig. 12. Online results of the 72-target system (a) accuracy (b) ITR.

the stimulus presentation was over, the system will process and analyzed the subject's EEG data. In the visual feedback stage, the stimuli square of judgment result was rendered blue and presented for 0.5s. The rest time between blocks was 2 minutes.

2) Data Acquisition and Analysis: In the Experiment D-Online, data of Experiment C-Offline was used in the training stage. The data preprocessing is the same as described in section III.B. The processed data was applied to the TS-TRCA algorithm, and the spatial filters and personal templates of 72-target systems were trained for target recognition in online experiments.

C. Experiment Results

1) Encoding Scheme: Generally, to increase the number of codewords in a code set, it is often necessary to sacrifice the distinguishability between different targets. Using the MSTDC method can expand the code set by increasing the length of the code, guaranteeing the distinguishability between the code words. Each codeword in the code set contained 72 targets used 5-bit symbol encoding. After adding one-bit symbol, the minimum code distance of the 72-target code set maintained the same level as the minimum code distance of the 40-target code set. The average distance between codewords is further increased by 23.4% (959.49→1184.13).

2) Online Experiments: According to the data of forty target stimulus offline experiments, the TS-TRCA method was used to construct classification templates of 72 targets. The results of the Experiment D-Online online experiment are shown in Fig. 12. After using the TS-TRCA method to build the classification template, twelve subjects achieved average recognition accuracy of 86.23%±7.75% and an average ITR of 95.68±14.19 bits/min in online experiments.

From comparing Fig. 9 and Fig. 12, the recognition performance of most subjects in the 72-targets system reduced significantly. On the one hand, increasing the number of targets leads to a decrease in the recognition probability. On the other hand, because the personal templates were derived from the symbol splicing of the offline data when the training data is sufficient, there is still a slight gap between the performance of TS-TRCA and the recognition performance of standard TRCA. The impact of training data on TS-TRCA will be further discussed in section VI.C.

VI. Discussions

A. Length of Symbols

Some TSR may occur when the process of initiating stimuli [21] and the switch between symbols. While TSR are evoked by user's gaze shift between stimuli and have no connection with code word. As a result, TSR are supposed to be the interference component. Whereas, by extending the duration of symbol stimulation, the negative influence of TSR towards classification can be decreased.

Considering the classification performance, participants show differences among suitability with symbol stimuli of different lengths. For some subjects, their TSR is longer, so their VEPs reach the steady-state slowly because of the smearing phenomenon. Their steady-state responses (SSR) components are weaker; a long time is used for the accumulation of adequate SSR energy. For those not good enough subjects, longer symbols are essential for ensuring the higher accuracy of every symbol.

It is worth mentioning that MSTDC enlarges the internal distances of code set by prolonging the length of codewords or adding redundancy. Consequently, the theoretical limit of its ITR cannot be higher than the ITR of a single symbol. Applying MSTDC can increase the number of targets or accuracy, but it cannot bring too much assistance for promoting ITR.

B. The Difference and the Correlation Between Codeword Response and Hamming Distance

In the area of communication, hamming distance is usually the primary evaluation index of codeword distance. It was defined as the number of different characters between two codewords in a same position. In the traditional communication system, larger the hamming distance, larger the distinguishability is. However, in the BCI system, hamming distance is not the most favorable criteria of code word distinguishability. Because the human brain responses specifically towards different stimulation; so selecting the hamming distance as the estimation of distinguishability ignores the divergence between symbol responses, which brings negative influence on classification.

According to our definition of the codeword response distance, this definition takes both hamming distance and the codeword divergence into consideration simultaneously. In this study, symbols were defined as the responses evoked by stimuli of different targets, and the symbol distance depends on the discrepancy between symbol responses. MSTDC selects the optimal code set by optimizing the arrangements of symbols, which maximizes the divergence between codeword responses. Future works may focus on designing specific code set for different subjects by utilizing the individual dataset.

C. Performance Comparison Between TS-TRCA and Standard TRCA

Many studies have tried various methods to reduce the training cost of SSVEP-based BCI [24]. Thanks to the time division coding method, MSTDC can significantly decrease the length of training data. To be more specific, MSTDC

TABLE IV
CLASSIFICATION ACCURACY OF ALL SUBJECTS IN TS-TRCA AND STANDARD TRCA (%)

Subjects		S1	S2	S3	S4	S5	S6	S7	S8	S9	S10	S11	S12	Mean	Std
TS-TRCA	1 block	85.00	85.00	85.31	91.25	98.44	95.00	92.19	97.19	97.50	91.25	91.25	93.13	**91.88**	4.80
	2 blocks	86.25	85.63	85.63	91.25	98.75	95.63	92.50	97.92	97.50	92.50	91.04	92.92	92.29	4.67
	3 blocks	85.94	86.56	85.31	91.25	98.75	95.94	93.13	97.81	97.50	92.19	90.94	93.44	92.40	4.66
	4 blocks	85.00	86.25	83.75	91.25	98.75	96.25	93.75	97.50	97.50	93.75	91.25	92.50	92.29	5.05
Standard TRCA	1 block	77.19	69.38	84.38	91.88	90.31	51.25	69.69	28.75	83.13	71.56	83.13	72.19	**72.73**	17.75
	2 blocks	91.46	88.75	98.54	95.42	99.58	91.88	96.04	84.58	95.83	93.13	93.75	93.75	93.56	4.12
	3 blocks	91.88	90.31	99.38	96.25	100.00	95.31	97.50	96.56	96.88	95.94	96.25	95.94	96.02	2.71
	4 blocks	92.50	92.50	100.00	96.25	100.00	95.00	97.50	97.50	98.75	96.25	97.50	97.50	96.77	2.47

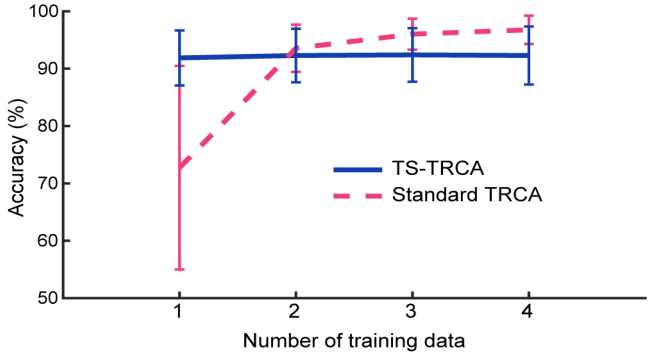

Fig. 13. Comparison of TS-TRCA and standard TRCA based on different number of training data (Experiment C-Offline dataset).

is an approach that encodes a large number of codewords through the repeated combination of limited symbols. Taking advantage of those finite symbols, experimental paradigms based on MSTDC only need to collect few blocks of EEG signals as the training dataset.

During the process of collecting Experiment C-Offline dataset, we test the detection performance of TS-TRCA and standard TRCA under the conditions that 1-4 blocks of training data were used for cross-validation. The results are presented in Table IV. It can be easily found that TS-TRCA achieved higher accuracy (91.88%±4.8%) than standard TRCA (72.73%±17.75%) when only one block of training data was used (p-value = 0.0059, paired t-test). Typically, S8 enhances its accuracy by almost 70%, probably caused by the instability of a single block of training data. After the template splicing strategy was introduced, the stability of training data was improved because the average times of symbol templates are much higher than codeword templates. With the growth in the number of training data, the growth rate of detection performance is more notable in standard TRCA. When more than two blocks of training data were implemented, the performance of standard TRCA was better than TS-TRCA. It should be pointed out that the accuracy acquired by TS-TRCA with one block training data has no significance compared with standard TRCA under two-block training data (p-value = 0.3609, paired T-test).

Each symbol in the training data appears 35-44 times in a block (a single block contains 40 trials, and each trial contains 4 symbols), so only a few blocks need to obtain a stable symbol response template. It can be seen from Fig. 13 that the promotion of accuracy caused by the increasing number of training blocks is not significant. In other words, the stability of splicing templates satisfied the requirements with only a few blocks, so MSTDC may play an essential role in reducing the training costs of SSVEP-based BCI.

D. Compare With Previous High-Frequency SSVEP-Based BCI Studies

Table V summarizes some of the recent studies on high-frequency SSVEP-based BCI. As can be seen in the table, most of the high-frequency SSVEP-based BCIs have few targets, and the information transfer rate is relatively low. Among them, the speller system reported in [14] achieves the highest number of target, and the system reported in [26] gets the highest ITR. But there are still some gaps in their performance compared with the 40-target and 72-target systems constructed in this study (72 targets vs 45 targets, 119.05 bits/min vs 87.2 bits/min). The comparison results show that substantial progress has been made in the multi-target high-frequency SSVEP-based BCI system constructed in this study, both in terms of target number and information transfer rate.

E. Possible Problems

As a time-division coding scheme, the MSTDC method usually needs to rely on high-precision clock synchronization in practical applications. The low precision of the clock may severely impact the detection efficiency of the paradigm, especially the high-frequency stimulation paradigm. Therefore, developing the stimulation paradigm composed of the MSTDC method must ensure that the stimulus code has a relatively high operating efficiency and low logic complexity.

In the authors' experience, stimulation programs clocked with frame intervals tend to achieve higher clock accuracy than those developed based on timers. For example, in this study, if it is necessary to generate a symbol target lasting 0.5s, a better option is to generate a stimulus lasting 120 frames in the stimulus code rather than set a stimulus to hold for 0.5s through a timer. If the timing control is performed in units of frames, the program mainly depends on the internal clock of the display; while the timer is used as the timing control, the program depends on the host clock. Although the display clock is synchronized with the host clock in most cases, the displayed stimulus may be "dropped" in the case of complex interfaces. At this time, the stability of the stimulus program

TABLE V
A COMPARISON OF HIGH-FREQUENCY SSVEP-BASED BCIS

Citation	Year	Target number	Subject number	Frequency (Hz)	Training Cost (s)	Trial Time (s)	Accuracy (%)	ITR (bits/min)
[14]	2014	45	10	35.6-44.4	0	4*	88.7	61
[15]	2015	6	3	25, 33.33, 40	0	1.9*	92	43
[22]	2018	8	15	30-39	480	6	96	47
[16]	2019	4	10	60	400	4*	92.71	18.81
[25]	2020	6	11	30	0	/	89.0	36.5
[26]	2020	10	4	31-40	0	1.5	87.5	87.2
ours	2021	40	12	30	480	3	96.77	119.05
		72	12	30	480	3.5	86.23	95.68

* Only including stimulation time.

TABLE VI
A COMPARISON BETWEEN THE RELATED WORKS

Features	MFSC in [11]	SSVEP-based BCI with 160 targets in [27]	MSTDC (this work)
Frequency coding?	Yes	Yes	No
Phase coding?	No	No	Yes
Temporal coding?	Yes	Yes	Yes
High frequency?	No	No	Yes
Num. of targets	4	160	40 or 72

relying on the display clock will be significantly better than a program for the host clock.

F. Relationship With Previous Studies

MFSC proposes a scheme of using different frequencies as stimulus symbols and using time-division coding to achieve multi-target stimulation [11]. Referring to this idea, this study proposes code set optimization criteria and optimization methods, and uses phase encoding to achieve 40-target and 72-target SSVEP-based BCI systems under the condition of 30Hz high-frequency stimulation. In addition to the above-mentioned references, the MSTDC method proposed in this study has been applied to the paradigm design of multi-target training-free SSVEP-based BCI. The authors use the MSTDC method to optimize the paradigm code set, implementing a calibration-free SSVEP-based BCI system with 160 targets [27]. The experimental results show that under the SSVEP paradigm of 160 candidate targets, the optimized code set based on MSTDC also has good performance. A comparison of relevant research contents is shown in Table VI.

VII. CONCLUSION & FUTURE WORKS

This study proposed MSTDC and an optimized encoding strategy based on response templates. In detail, this study achieved an SSVEP-based BCI containing forty targets, with encoding symbols of four phases. The effectiveness of the optimization strategy was validated through offline experiments. In the online experiments of the forty targets system, the encoding scheme based on the optimized strategy acquired an average accuracy of 96.77%±2.47% and an average ITR of 119.05±6.11 bits/min. Moreover, this study also proposed TS-TRCA that corresponds to the system based on MSTDC. In the offline analysis section, this study validated the feasibility of MSTDC and TS-TRCA in the multi-targets SSVEP-based BCI, with less training data. Because the symbol can be expanded into other areas. As a result, by combining different kinds of symbols, MSTDC is hopefully applied in other evoked BCI paradigms such as SSVEP; code modulated visual evoked potentials (C-VEP); motion-related visual evoked potential (M-VEP); P300; auditory steady-state response (ASSR); etc.

In future work, the potential of MSTDC can be exploited through expanding symbols, optimizing symbols or training optimization. First of all, symbols in MSTDC can be extended to other evoked potentials (EP) or event-related potentials (ERP) through combining different symbols with building multi-targets SSVEP-based BCI. Furthermore, overall ITR can be further enhanced by optimizing the length of symbols or shortening the stimulation duration. Finally, the training cost of this system can be reduced for better usability of BCI systems.

ACKNOWLEDGMENT

The authors would like to thank Jiang Lu for providing the calibration dataset. Xiaochen Ye is responsible for algorithm implementation, data processing, and picture drawing. Chen Yang is responsible for method proposal, experimental design, and paper writing.

REFERENCES

[1] S. Gao, Y. Wang, X. Gao, and B. Hong, "Visual and auditory brain-computer interfaces," *IEEE Trans. Biomed. Eng.*, vol. 61, no. 5, pp. 1436–1447, May 2014.
[2] M. Zhuang, Q. Wu, F. Wan, and Y. Hu, "State-of-the-art non-invasive brain–computer interface for neural rehabilitation: A review," *J. Neurorestoratol.*, vol. 8, no. 1, pp. 12–25, Mar. 2020.
[3] N. Shi *et al.*, "Steady-state visual evoked potential (SSVEP)-based brain–computer interface (BCI) of Chinese speller for a patient with amyotrophic lateral sclerosis: A case report," *J. Neurorestoratol.*, vol. 8, no. 1, pp. 40–52, Mar. 2020.
[4] D. Regan, *Human Brain Electrophysiology: Evoked Potentials and Evoked Magnetic Fields*. New York, NY, USA: Elsevier, 1989.
[5] Y. S. Zhang *et al.*, "Two-stage frequency recognition method based on correlated component analysis for SSVEP-based BCI," *IEEE Trans. Neural Syst. Rehabil. Eng.*, vol. 26, no. 7, pp. 1314–1323, Jul. 2018.

[6] E. Yin, Z. Zhou, J. Jiang, Y. Yu, and D. Hu, "A dynamically optimized SSVEP brain-computer interface (BCI) speller," *IEEE Trans. Biomed. Eng.*, vol. 62, no. 6, pp. 1447–1456, Jun. 2015.

[7] Y. Zhao, H. Zhang, Y. Wang, C. Li, R. Xu, and C. Yang, "An extended binary subband canonical correlation analysis detection algorithm oriented to the radial contraction-expansion motion steady-state visual evoked paradigm," *Brain Sci. Adv.*, vol. 8, no. 1, pp. 19–37, Mar. 2022.

[8] S. Zhang, J. Sun, and X. Gao, "The effect of fatigue on brain connectivity networks," *Brain Sci. Adv.*, vol. 6, no. 2, pp. 120–131, Jun. 2020.

[9] C. Yang, X. Han, Y. Wang, R. Saab, S. Gao, and X. Gao, "A dynamic window recognition algorithm for SSVEP-based brain–computer interfaces using a spatio-temporal equalizer," *Int. J. Neural Syst.*, vol. 28, no. 10, Dec. 2018, Art. no. 1850028.

[10] X. Chen, Y. Wang, M. Nakanishi, T.-P. Jung, and X. Gao, "Hybrid frequency and phase coding for a high-speed SSVEP-based BCI speller," in *Proc. 36th Annu. Int. Conf. IEEE Eng. Med. Biol. Soc.*, Aug. 2014, pp. 3993–3996.

[11] Y. Zhang, P. Xu, T. Liu, J. Hu, R. Zhang, and D. Yao, "Multiple frequencies sequential coding for SSVEP-based brain-computer interface," *PLoS ONE*, vol. 7, no. 3, Mar. 2012, Art. no. e29519.

[12] M. A. Pastor, J. Artieda, J. Arbizu, M. Valencia, and J. C. Masdeu, "Human cerebral activation during steady-state visual-evoked responses," *J. Neurosci.*, vol. 23, pp. 11621–11627, Dec. 2003.

[13] U. Hoffmann, E. J. Fimbel, and T. Keller, "Brain-computer interface based on high frequency steady-state visual evoked potentials: A feasibility study," in *Proc. 4th Int. IEEE/EMBS Conf. Neural Eng.*, Apr. 2009, pp. 466–469.

[14] X. Chen, Z. Chen, S. Gao, and X. Gao, "A high-ITR SSVEP-based BCI speller," *Brain-Comput. Interfaces*, vol. 1, nos. 3–4, pp. 181–191, Oct. 2014.

[15] F. Zhang *et al.*, "High-frequency combination coding-based steady-state visual evoked potential for brain computer interface," in *Proc. AIP Conf.*, vol. 1648, 2015, Art. no. 850136.

[16] L. Jiang, Y. Wang, W. Pei, and H. Chen, "A four-class phase-coded SSVEP BCI at 60Hz using refresh rate," in *Proc. 41st Annu. Int. Conf. IEEE Eng. Med. Biol. Soc. (EMBC)*, Jul. 2019, pp. 6331–6334.

[17] E. Erkut, "The discrete p-dispersion problem," *Eur. J. Oper. Res.*, vol. 46, no. 1, pp. 48–60, May 1990.

[18] B. Hajek, "A tutorial survey of theory and applications of simulated annealing," in *Proc. 24th IEEE Conf. Decis. Control*, Dec. 1985, pp. 755–760.

[19] N. V. Manyakov, N. Chumerin, A. Robben, A. Combaz, M. van Vliet, and M. M. Van Hulle, "Sampled sinusoidal stimulation profile and multichannel fuzzy logic classification for monitor-based phase-coded SSVEP brain–computer interfacing," *J. Neural Eng.*, vol. 10, no. 3, Jun. 2013, Art. no. 036011.

[20] M. Nakanishi, Y. Wang, X. Chen, Y.-T. Wang, X. Gao, and T.-P. Jung, "Enhancing detection of SSVEPs for a high-speed brain speller using task-related component analysis," *IEEE Trans. Biomed. Eng.*, vol. 65, no. 1, pp. 104–112, Jan. 2018.

[21] S. Zhang, X. Han, X. Chen, Y. Wang, S. Gao, and X. Gao, "A study on dynamic model of steady-state visual evoked potentials," *J. Neural Eng.*, vol. 15, no. 4, Aug. 2018, Art. no. 046010.

[22] A. Chabuda, P. Durka, and J. Zygierewicz, "High frequency SSVEP-BCI with hardware stimuli control and phase-synchronized comb filter," *IEEE Trans. Neural Syst. Rehabil. Eng.*, vol. 26, no. 2, pp. 344–352, Feb. 2018.

[23] X. Chen, Y. Wang, S. Gao, T.-P. Jung, and X. Gao, "Filter bank canonical correlation analysis for implementing a high-speed SSVEP-based brain–computer interface," *J. Neural Eng.*, vol. 12, no. 4, Aug. 2015, Art. no. 046008.

[24] C. M. Wong *et al.*, "Learning across multi-stimulus enhances target recognition methods in SSVEP-based BCIs," *J. Neural Eng.*, vol. 17, no. 1, Jan. 2020, Art. no. 016026.

[25] X. Mao, W. Li, H. Hu, J. Jin, and G. Chen, "Improve the classification efficiency of high-frequency phase-tagged SSVEP by a recursive Bayesian-based approach," *IEEE Trans. Neural Syst. Rehabil. Eng.*, vol. 28, no. 3, pp. 561–572, Mar. 2020.

[26] L. Yue *et al.*, "A brain-computer interface based on high-frequency steady-state asymmetric visual evoked potentials," in *Proc. 42nd Annu. Int. Conf. IEEE Eng. Med. Biol. Soc. (EMBC)*, Jul. 2020, pp. 3090–3093.

[27] Y. Chen, C. Yang, X. Ye, X. Chen, Y. Wang, and X. Gao, "Implementing a calibration-free SSVEP-based BCI system with 160 targets," *J. Neural Eng.*, vol. 18, no. 4, Jun. 2021, Art. no. 046094.